

# Grain growth at the free surface of WC-Co materials

J. M. OLSON, M. M. MAKHLOUF

*Department of Mechanical Engineering, Worcester Polytechnic Institute, Worcester, Massachusetts, USA*

The grain growth rate at the free surface of a WC-Co material was measured at different high temperatures and the microstructure and elemental composition of the material were characterized at various stages of the grain growth process. It was found that free surface grains grew at an abnormally fast rate, and this fast growth rate coincided with the vaporization of the binder phase from the free surface. It is suggested that this abnormal rate of growth is related to a change in the growth mechanism from interfacial reaction limited growth in the bulk of the material to a surface diffusion rate limited growth at the free surface. It is shown that the contact points between grains provide bridges for atomic transport from the high free-energy regions (the small grains) to the low free-energy regions (the large grains); hence, the contiguity of the material strongly influences the rate of growth. It is believed that vaporization of the binder phase allows for an increased atomic mobility at the surface, a reduction in the energy barrier to chemisorption and consequently an accelerated grain growth. © 2001 Kluwer Academic Publishers

## 1. Introduction

Continued efforts to produce a diamond film/WC-Co material with enhanced characteristics led to novel surface modification techniques that are specifically designed to improve adhesion between WC-Co substrates and thin diamond films. One such surface modification technique relies on simultaneous controlled vaporization of the binder phase and rapid growth of the WC grains at the surface. The resultant grain size and morphology of the WC phase at the surface enhance the deposition rate of diamond on the WC-Co substrate and result in a strong adherent film. While the superiority of this process has been demonstrated [1], a fundamental understanding of the mechanism that governs the evolution of the desirable surface characteristics of the WC-Co substrate is yet to be attained. In this publication, the grain growth at the surface of a typical WC-Co substrate material is characterized and a mechanism is proposed to explain the observed abnormal grain growth rate.

## 2. Background

Grain growth is driven by a reduction in the surface free energy associated with the grain boundaries of the system [2–5], and the grain growth law may be written as

$$(D^2 - D_0^2)/t = K_0 e^{-Q/RT} \quad (1)$$

In Equation 1,  $D$  is the mean grain diameter after some time  $t$ ,  $D_0$  is the initial grain diameter,  $K_0$  is a constant, and  $Q$  is the activation energy for the process. Taking the natural logarithm of both sides of Equation 1

yields

$$\ln((D^2 - D_0^2)/t) = \ln K_0 - Q/RT \quad (2)$$

Examination of Equation 2 shows that a plot of  $\ln((D^2 - D_0^2)/t)$  vs.  $1/T$  is linear with a slope of  $-(Q/R)$  and a  $y$ -intercept that yields the constant  $K_0$ . Wagner [4] showed that in the case of interface-controlled Ostwald ripening, the grain growth rate depends linearly on the driving force, which is determined by the grain size difference. It is predicted that the system will eventually reach a steady state where the normalized grain size distribution remains invariant. This grain size distribution is predicted to be relatively narrow with the largest grain about 2.25 times larger than the average grain [6]. Abnormal growth of grains dispersed in a matrix may be defined as the case where the grain size distribution becomes wider than that predicted by the usual Ostwald ripening theories, and where geometrical self-similarity may be violated. Although the size distribution of grains with complex shapes is usually difficult to determine, a small fraction of the grains is sometimes observed to be so much larger than the rest that abnormal growth can be unambiguously identified [7].

In this publication, the grain growth rate of the WC phase at the surface of a WC-6%Co material is characterized. The grain growth rate constant and activation energy for grain growth are determined and compared to their counterparts for bulk grain growth in this class of materials. A mechanism is proposed to explain the thermodynamic and kinetic differences between the evolution of the microstructure of the WC phase at the free surface and within the bulk of WC-Co materials.

TABLE I Grain size of the WC phase in the bulk of samples that were heat-treated for 45 minutes at various temperatures

Temperature (°C)	No. of Grains	
	Measured	$D_{avg}$ ( $\mu\text{m}$ )
1350	153	1.109
1400	117	1.113
1450	191	1.164
1500	160	1.327
1550	111	1.209
1600	134	1.438
1650	152	1.969

### 3. Materials and procedures

The samples used were 94 wt% WC-6 wt% Co commercial WC-Co inserts.\* The average grain size of the WC phase was between 1 to 2  $\mu\text{m}$ , and the free-carbon concentration in the samples was 10.9  $\mu\text{Tm}^3/\text{kg}$ .<sup>†</sup>

Prior to each isothermal heat treatment, the samples were laser scribed with individual identification marks and weighed.<sup>‡</sup> Then they were placed on a graphite plate inside an atmosphere furnace and the temperature within the furnace was increased at a rate of 20°C/minute until the test temperature was reached. The specimens were heat-treated for 45 minutes at each of 1350°C, 1400°C, 1450°C, 1500°C, 1550°C, and 1600°C.

Following each heat-treatment cycle, the final mass of the samples was recorded and mass loss due to vaporization of the binder phase was calculated. X-ray diffraction (XRD) was used to characterize the phase composition of the samples, and scanning electron microscopy (SEM) and energy dispersive spectroscopy (EDS) were used to characterize the microstructure and to determine the grain-size and the composition of the WC phase at the free-surface and in the bulk of the samples. In addition, Field Emission Scanning Electron Microscopy<sup>§</sup> was used to examine the microstructural changes in the WC phase at the free surface of the samples. The system was equipped with an energy dispersive x-ray analyzer which was operated in scan, dot map, and spot modes in order to identify the composition of particular features of interest.

## 4. Results and discussion

### 4.1. Grain growth in the bulk

Fig. 1a through h show SEM photomicrographs of the samples in the as-received condition as well as after heat treatment for 45 minutes at 1350°C, 1400°C, 1450°C, 1500°C, 1550°C, 1600°C and 1650°C, respectively. Table I summarizes the results of the grain size analysis in the bulk of the samples. Fig. 2 shows the variation of  $\ln\{(D^2 - D_0^2)/t\}$  with  $1/T$  and is used to calculate the activation energy for grain growth of the WC within the bulk of the WC-Co samples,  $Q_{\text{bulk}} = 98$  kcal/mol. This magnitude of  $Q_{\text{bulk}}$  compares well with published values [8–12].

\* Manufactured by Sandvik Coromant.

† Determined from magnetic saturation measurements.

‡ Using a Mettler AE50 microbalance.

§ An ABT model 150F.

TABLE II Grain size of the WC phase at the free surface of samples that were heat-treated for 45 minutes at various temperatures

Temperature (°C)	$\Delta m_{\text{loss}}$ (%)	# of Grains	
		Measured	$D_{avg}$ ( $\mu\text{m}$ )
1350	0.03	206	0.730
1400	0.10	197	0.806
1450	0.21	209	0.881
1500	0.55	103	1.148
1550	2.67	78	7.459
1600	3.34	69	16.913

### 4.2. Grain growth at the surface

Table II summarizes the results of the mass change and grain size analysis at the surface of the samples.

Fig. 3, which is a graphical representation of the data presented in Table II, shows that there is a dramatic increase in grain size for heat-treating temperatures  $T \geq 1500^\circ\text{C}$ . This temperature is above the melting point of the binder phase, and since the vapor pressure of metals increases significantly at the onset of melting [13], it is believed that the increase in the growth rate at  $T \geq 1500^\circ\text{C}$  corresponds to vaporization of the binder phase from the surface. This is confirmed by the EDS images shown in Fig. 4.

Table II shows that samples that were heat-treated for 45 minutes at 1350°C lost 0.03% of their original weight upon heat-treating and the average grain size of the WC phase remained uniform. While some vaporization of the binder phase has occurred, a significant amount of Co remained at the free surface of the samples. Samples that were heat-treated for 45 minutes at 1400°C lost 0.10% of their original weight upon heat-treating and the average grain size of the WC phase increased but only slightly. While vaporization of the binder phase was observed, a significant amount of Co remained at the free surface of the samples, especially at the grain boundaries of the WC grains. Samples that were heat-treated for 45 minutes at 1450°C lost 0.21% of their original weight upon heat-treating and the increase in average grain size of the WC phase was small. Again, while vaporization of the binder phase was observed, a significant amount of Co remained at the free surface, especially at the grain boundaries of the WC grains. Samples that were heat-treated for 45 minutes at 1500°C lost 0.55% of their original weight upon heat-treating. At this temperature, vaporization of the binder phase at the free surface appears more complete than at the lower temperatures, yet Co is still present at the grain boundaries of the WC grains as illustrated by the EDS dot-map image presented in Fig. 5. After heat-treating for 45 minutes at 1550°C, the rate of Co vaporization increased significantly and the samples showed an average weight loss of 2.67%. At this temperature, vaporization of the binder phase at the free surface appears to be complete and Co is not detected at the grain boundaries of the WC grains as illustrated in the EDS dot-map image presented in Fig. 6. The average grain size, which has increased significantly, appears to be uniform with a dominant trigonal morphology as illustrated in Fig. 7. After heat-treating for 45 minutes at 1600°C, the samples showed an average weight loss

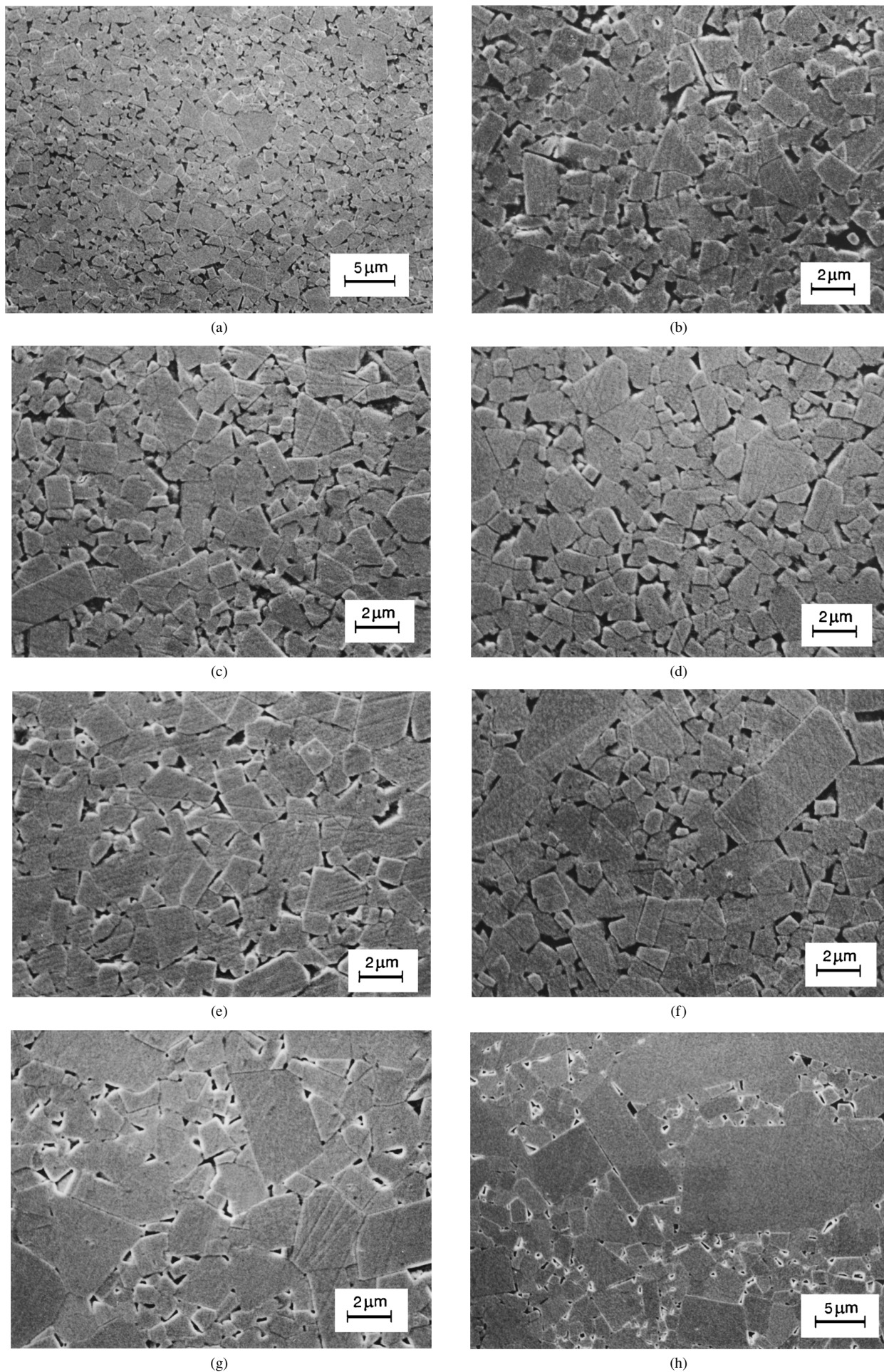


Figure 1 The grain structure of WC-6Co (a) as-received, (b) fired for 45 min. at 1350°C, (c) fired for 45 min. at 1400°C, (d) fired for 45 min. at 1450°C, (e) fired for 45 min. at 1500°C, and (f) fired for 45 min. at 1550°C. The grain structure of WC-6Co samples (g) fired for 45 min. at 1600°C and (h) fired for 45 min. at 1650°C.

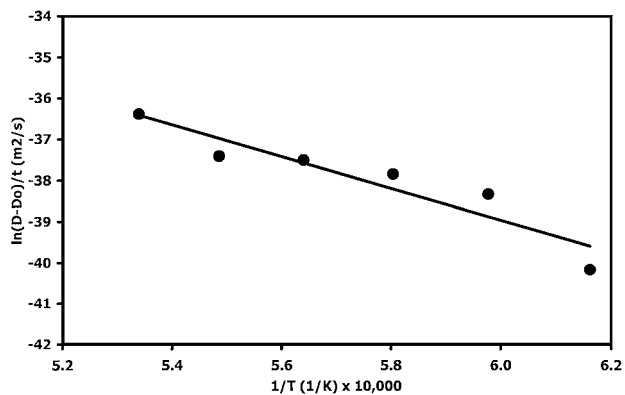


Figure 2 Variation of  $\ln\{(D^2 - D_0^2)/t\}$  with  $1/T$ .

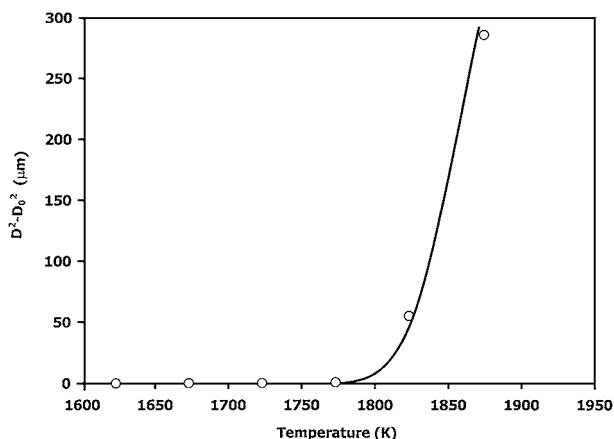


Figure 3 Growth of the WC phase at the surface of a WC-6%Co material depicted as change in  $(D^2 - D_0^2)$  with temperature.

of 3.34%. Fig. 8 shows that at this temperature, stratification of individual grains into thin parallel plates has occurred and the average grain size has increased significantly over that of samples heat-treated at lower temperatures.

Fig. 9 shows the variation of  $\ln\{(D^2 - D_0^2)/t\}$  with  $1/T$ . Fig. 9 shows that the activation energy for grain growth at the free surface,  $Q_{\text{surface}}$ , changes dramatically at  $T = 1500^\circ\text{C}$ . Treating the data as two separate sets,  $Q_{\text{surface}}$  is determined for  $T < 1500^\circ\text{C}$ , i.e., before binder vaporization to be 108 kcal/mol, and for  $T \geq 1500^\circ\text{C}$ , i.e., after binder vaporization to be 387 kcal/mol. The activation energy for grain growth in the bulk of this material is 98 kcal/mol, which is comparable to that for surface grain growth during its initial stages, i.e., before binder vaporization. However, the magnitudes of both the activation energy and the grain growth constant following binder phase vaporization are anomalous when compared to corresponding parameters for bulk grain growth.

In the preceding analysis, it is assumed that grain growth is an activated process and thus transport of material occurs across an energy barrier. According to this assumption, an increase in the growth rate at the surface is the consequence of a reduction in the magnitude of this energy barrier. Thus, the dramatic increase in the growth rate of WC grains at the free surface must be the consequence of a lower activation energy barrier.

However, since the calculated activation energy for free surface grain growth is considerably larger than

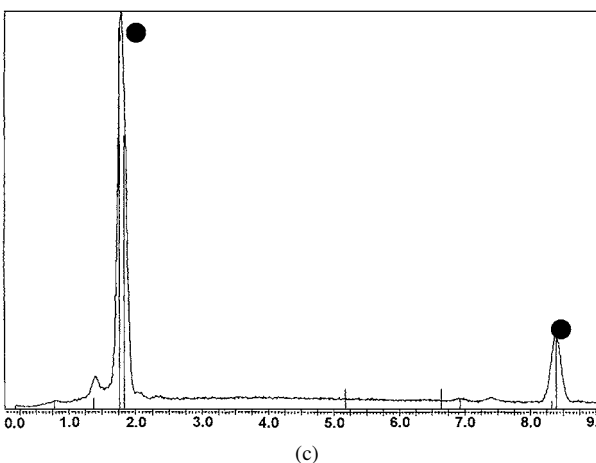
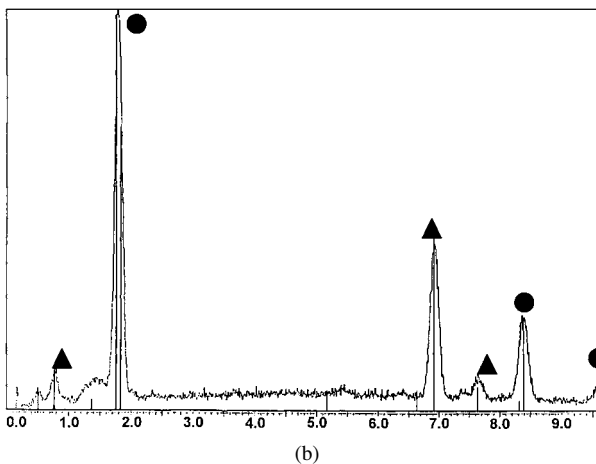
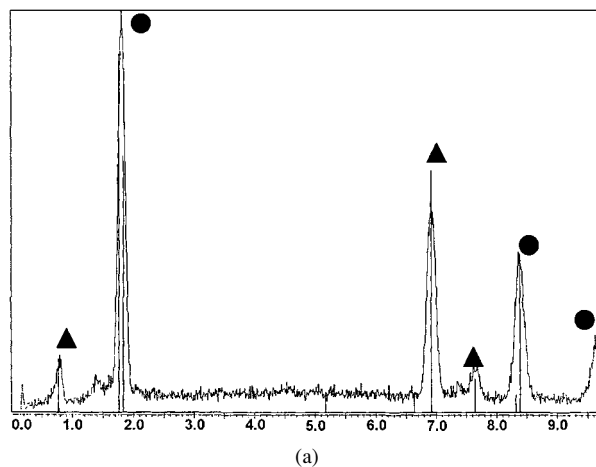
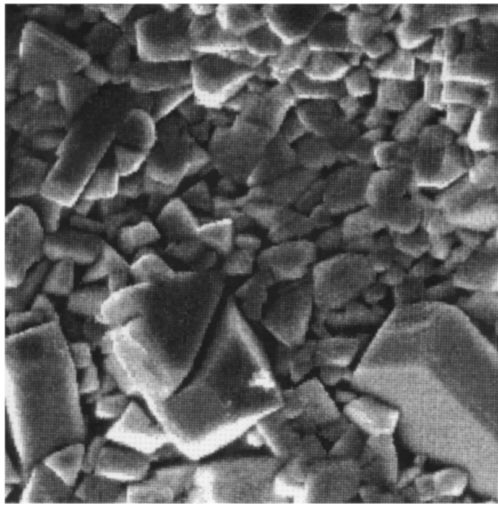


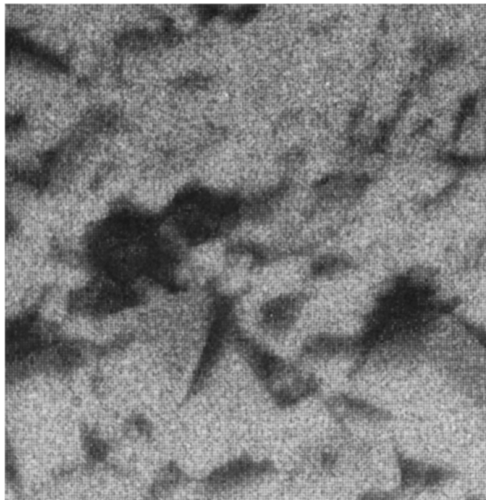
Figure 4 EDS spectra showing the rapid vaporization of Co from the surface of a WC-6%Co material upon heat-treatment. (a) Prior to heat treatment, (b) Heat treated at  $1450^\circ\text{C}$  for 45 minutes, (c) Heat treated at  $1550^\circ\text{C}$  for 45 minutes. ▲ Indicates a Co peak. ● Indicates a W peak.

the activation energy for bulk grain growth, we postulate that the use of Equation 2 is not appropriate for quantifying grain growth of WC at the free surface of these materials. Moreover, we suggest that several of the parameters that influence grain growth at the free surface of WC-Co materials are temperature dependent and undergo changes that are significant enough to cause a shift in the grain growth mechanism from interfacial reaction limited growth to surface diffusion limited growth.

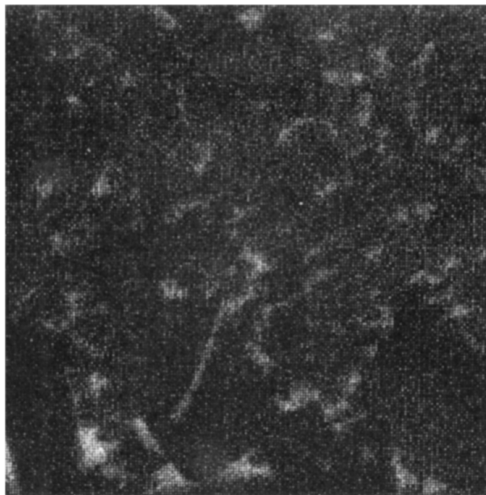
The free energy associated with the interface between a solid phase (S) and a liquid phase (L) in intimate



(a)



(b)



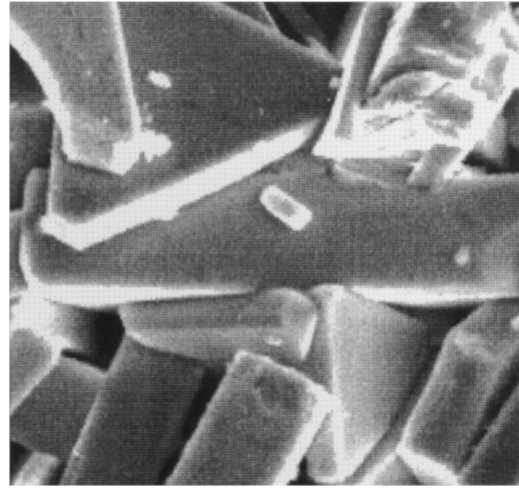
(c)

Figure 5 EDS dot map image of a WC-6%Co material heat-treated at 1500°C for 45 minutes. (a) Image, (b) tungsten, and (c) cobalt.

contact is given by Equation 3 [14]

$$\gamma_i = \gamma_{sv} - \gamma_{lv} \cos \theta \quad (3)$$

In Equation 3,  $\gamma_i$  is the interfacial free energy between the solid and liquid phases,  $\gamma_{sv}$  is the surface free energy of the solid/vapor interface,  $\gamma_{lv}$  is the surface free energy of the liquid/vapor interface and  $\theta$  is the contact angle as illustrated in Fig. 10. When the binder phase



(a)



(b)



(c)

Figure 6 EDS dot map image of a WC-6%Co material heat-treated at 1500°C for 45 minutes. (a) Image, (b) tungsten, and (c) cobalt.

in WC-Co materials is in the liquid phase, the binder phase completely wets the surface of the WC grains, so that  $\theta \approx 0$  and

$$\gamma_i \approx \gamma_{sv} - \gamma_{lv} \quad (4)$$

i.e.,

$$\gamma_i \approx \gamma_{wc} - \gamma_{co} \quad (5)$$

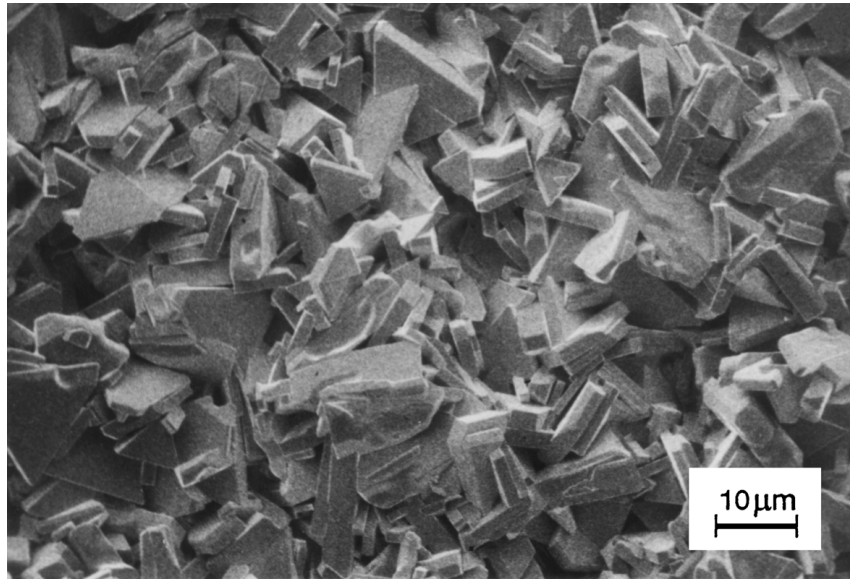


Figure 7 SEM photomicrograph of polished surface of sample heat-treated at 1550°C for 45 minutes.

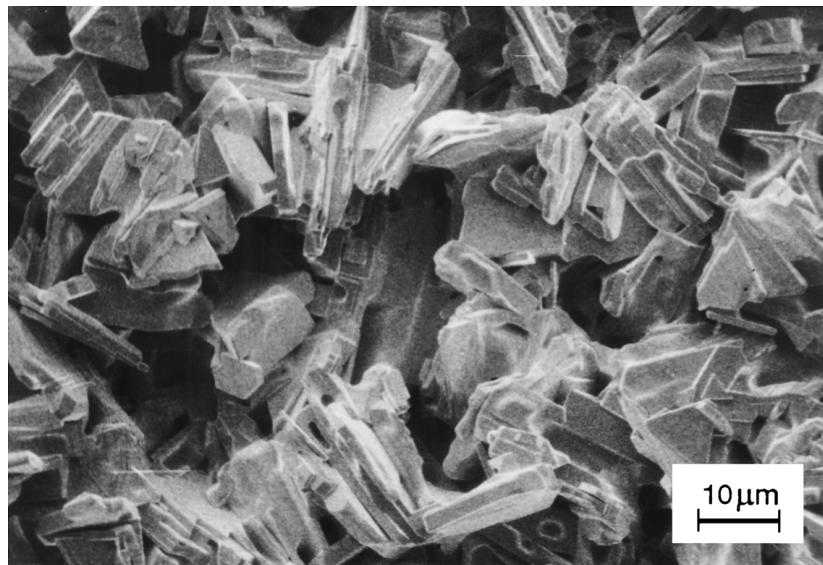


Figure 8 SEM photomicrograph of polished surface of sample heat-treated at 1600°C for 45 minutes.

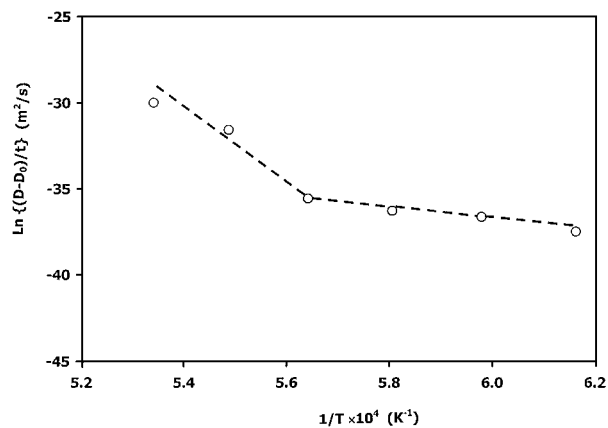


Figure 9 Variation of the quantity  $\ln\{(D^2 - D_0^2)/t\}$  with the reciprocal of temperature for WC grain growth at the surface of a WC-6%Co material.

In Equation 5,  $\gamma_{WC} = 2.460 \text{ Jm}^{-2}$  and  $\gamma_1 = 0.610 \text{ Jm}^{-2}$  [15]. The fact that the growth rate of WC grains at the surface of WC-Co substrates increases dramatically following the vaporization of the binder phase can be

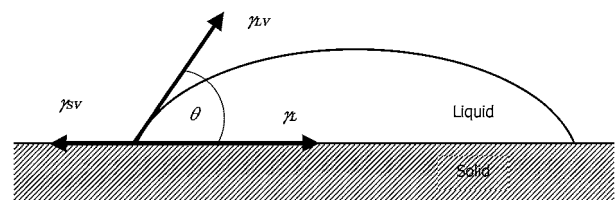


Figure 10 Schematic representation of a liquid droplet on a solid substrate.

explained by the fact that in the presence of Co, the interfacial free energy  $\gamma_1$  is equal to  $(\gamma_{WC} - \gamma_{Co})$  and upon vaporization of the binder phase, it is equal to  $\gamma_{WC}$ . This is an increase of  $1.85 \text{ Jm}^{-2}$ , which represents a relative increase in the surface free energy of more than 300%. Surface diffusion is generally more rapid than bulk diffusion due to the open structure that is characteristic of surfaces [5, 16]. The surface free energy may be simplistically viewed as proportional to the density of dangling bonds at the surface. These dangling bonds act as open sites for atomic hopping at the surface. Thus,

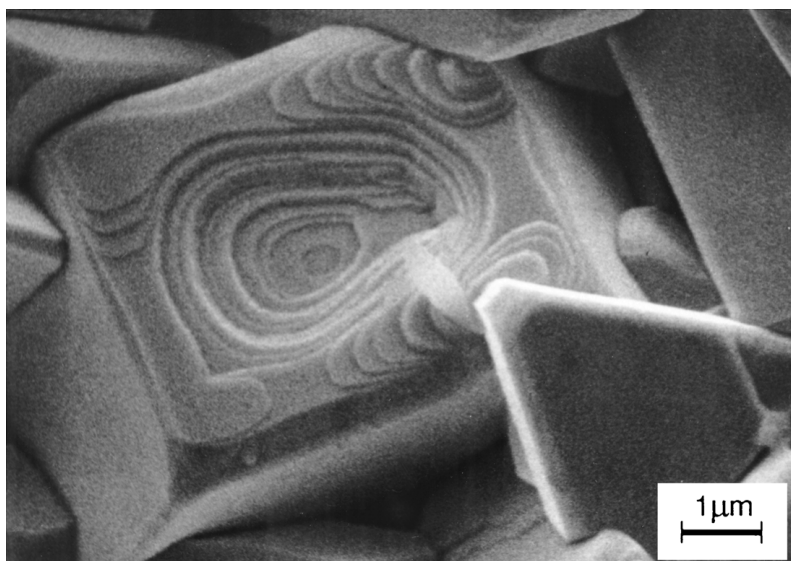


Figure 11 Convex growth steps at the surface of a WC-6%Co material after binder phase vaporization.

the increase in the surface free energy that results from vaporization of Co from the surface of the WC grains provides for an increase in the mobility of atoms diffusing along the surface compared to the mobility of atoms within the bulk of the material.

Fig. 11 provides further evidence that growth of the WC grains at the surface of WC-Co materials after binder vaporization occurs via a surface diffusion limited mechanism. Fig. 11 shows the free surface of a sample following vaporization of the free surface binder phase. At the surface of this sample, convex growth ledges are evident on the prismatic planes of many of the grains. The microstructure of the ledges implies that growth occurs by a mechanism in which material diffuses across contact points between grains and along the surface of a growing grain in the form of a growth "front".

## 5. Summary

The rate of grain growth at the free surface of WC-Co materials was characterized. The microstructure, phase evolution and elemental composition at the free surface were characterized at various stages of the grain growth process. It is observed that the rate of grain growth at the surface of these materials is much faster than in their bulk. It is postulated that this dramatic increase in the rate of growth of the WC phase at the surface coincides with the vaporization of the binder phase from the surface. Growth of the WC grains in the bulk of WC-Co materials has been studied extensively, and it is generally accepted that grain growth in these materials is limited by interfacial reactions. We propose that the fast rate of grain growth at the free surface of these materials is due to a change in the grain growth mechanism from interfacial reaction limited growth in the bulk to a surface diffusion

rate limited growth at the free surface. The identification of this grain growth mechanism should have important ramifications on many applications of these materials, particularly adhesion of coatings, e.g. diamond films, to WC-metal carbide-Co substrates, and on the development of methods and grain growth inhibitors to mitigate excessive grain growth in WC-metal carbide-Co alloys.

## References

1. J. M. PINEO, European Patent Application 93308250.5 (1993).
2. P. SCHWARZKOPF and R. KIEFFER, "Cemented Carbides" (Macmillan Company, New York, 1960).
3. H. E. EXNER, *Intl. Met. Rev.* **4** (1979) 149.
4. C. WAGNER, *Z. Elektrochem* **65** (1961) 581.
5. D. A. PORTER and K. E. EASTERLING, "Phase Transformations in Metals and Alloys" (Chapman & Hall, 1992).
6. C. V. THOMPSON, H. J. FROST and F. SPAEPAN, *Acta Metal.* **35** (1987) 887.
7. P. G. SHEWMON, "Transformations in Metals" (McGraw-Hill, 1969).
8. L. SKOLNICK, "Kinetics of High Temperature Processes" (MIT and Wiley, 1959).
9. H. E. EXNER and H. FISCHMEISTER, *Z. Metallkde* **57** (1966) 187.
10. *Idem.*, *Arch Eisenhut.* **37**(5) (1966) 417.
11. M. COSTER and A. DESCHANVRES, *Compt. Rend.* **296** (1969) 291.
12. J. L. CHERMANT, M. COSTER, A. DESCHANVRES and A. IOST, *J. of Less-Common Mtls.* **52** (1977) 177.
13. D. R. GASKELL, "Introduction to Thermodynamics of Materials," 3rd Ed. (Taylor and Francis, 1995).
14. K. REICHEL, *Vacuum* **38** (1988) 1083.
15. R. WARREN, *J. Mater. Sci.* **15**(10) (1980) 2489.
16. R. E. REED-HILL and R. ABBASCHIAN, "Physical Metallurgy Principles," 3rd ed. (PWS Publishing Company, 1994).

Received 15 March  
and accepted 26 December 2000